M2+ ions bind at the C-terminal region of skeletal muscle α-tropomyosin

ARTICLE *in* BIOPOLYMERS · JULY 2009

Impact Factor: 2.39 · DOI: 10.1002/bip.21185 · Source: PubMed

3 AUTHORS, INCLUDING:

Fernando Correa
University of Texas Southwestern Medical Center
13 PUBLICATIONS **86** CITATIONS
SEE PROFILE

Chuck Farah
University of São Paulo
68 PUBLICATIONS **2,011** CITATIONS
SEE PROFILE

Mg^{2+} Ions Bind at the C-Terminal Region of Skeletal Muscle α-Tropomyosin

Fernando Corrêa, Chuck S. Farah, Roberto K. Salinas
Departamento de Bioquímica, Instituto de Química, Universidade de São Paulo, São Paulo, SP, Brazil

Received 23 September 2008; revised 13 February 2009; accepted 27 February 2009
Published online 11 March 2009 in Wiley InterScience (www.interscience.wiley.com). DOI 10.1002/bip.21185

ABSTRACT:

Tropomyosin (Tm) is a dimeric coiled-coil protein that polymerizes through head-to-tail interactions. These polymers bind along actin filaments and play an important role in the regulation of muscle contraction. Analysis of its primary structure shows that Tm is rich in acidic residues, which are clustered along the molecule and may form sites for divalent cation binding. In a previous study, we showed that the Mg^{2+}-induced increase in stability of the C-terminal half of Tm is sensitive to mutations near the C-terminus. In the present report, we study the interaction between Mg^{2+} and full-length Tm and smaller fragments corresponding to the last 65 and 26 Tm residues. Although the smaller Tm peptide ($Tm_{259\text{-}284(W269)}$) is flexible and to large extent unstructured, the larger $Tm_{220\text{-}284(W269)}$ fragment forms a coiled coil in solution whose stability increases significantly in the presence of Mg^{2+}. NMR analysis shows that Mg^{2+} induces chemical shift perturbations in both $Tm_{220\text{-}284(W269)}$ and $Tm_{259\text{-}284(W269)}$ in the vicinity of His276, in which are located several negatively charged residues. © *2009 Wiley Periodicals, Inc. Biopolymers 91: 583–590, 2009.*

Correspondence to: Chuck S. Farah; e-mail: chsfarah@iq.usp.br or Roberto K. Salinas; e-mail: Roberto@iq.usp.br
F. C. is a FAPESP graduate fellow and R. K. S. is the recipient of an Young Scientist Fellowship from FAPESP.
Contract grant sponsor: Fundação de Amparo à Pesquisa do Estado de São Paulo (FAPESP)

Keywords: *tropomyosin; coiled-coil; muscle-thin filament; nuclear magnetic resonance; protein stability*

This article was originally published online as an accepted preprint. The "Published Online" date corresponds to the preprint version. You can request a copy of the preprint by emailing the Biopolymers editorial office at biopolymers@wiley.com

INTRODUCTION

Magnesium ions are encountered ubiquitously in all cellular compartments and play a role as a cofactor essential for the function of many proteins. This is the case for many of the components of the skeletal muscle thin filament.[1–5] Under relaxed conditions, the structure of the troponin (Tn) complex is stabilized by Mg^{2+} binding to two carboxy domain EF-hand sites in TnC (sites III and IV).[1–3] Mg^{2+} is also necessary for the polymerization of actin.[5]

Tropomyosin (Tm) is an α-helical coiled-coil protein composed of 284 residues (410 Å). Tm N- and C-terminal ends interact through head-to-tail interactions to form long linear polymers that lie along each of the two strands of the actin helix.[6–8] The Tm coiled-coil results from a series of heptapeptide repeats (*abcdefg*) along its entire primary structure where hydrophobic residues at positions *a* and *d* are hidden from the solvent by forming a dimerization interface, while residues at other positions are solvent-exposed and tend to be hydrophilic. Analysis of the chemical nature of solvent-exposed residues demonstrated that Tm can be subdivided into seven alternative α and β bands which each have a narrow zone of net-positive charge and a broader negatively charged zone.[9,10] Mg^{2+} has been shown to stabilize the binding of Tm to actin[11–13] and it has been suggested that Mg^{2+}

could mediate intermolecular salt bridges between negatively charged residues at the Tm-actin interface.[9,10,14]

In a previous study,[15] we showed that the presence of Mg^{2+} ions significantly increases the thermal stability of Tm fragments corresponding to both the N-terminal ($ASTm_{1-142}$) and the C-terminal halves ($Tm_{143-284}$) of the molecule. Interestingly, the Mg^{2+}-dependent gains in stability were highly sensitive to mutations at the extreme carboxi terminus of $Tm_{143-284}$ (Mg^{2+}-induced stability gain: H276E > H276A > wild-type > D275A > D280A), but were independent of mutations in the N-terminal fragment $ASTm_{1-142}$ (D2A, K5A, K6A, K7A). Though Mg^{2+} did not influence the stability of the wild-type head-to-tail complex, it modulated the stability of mutant complexes. These observations led us to hypothesize that one (or more) Mg^{2+} binding site(s) could be located at the Tm C-terminus next to or within the overlap region.[15]

In the present study, we show by limited proteolysis digestions and thermal denaturation experiments followed by CD spectroscopy, that the addition of Mg^{2+} increases the stability of a shorter recombinant fragment derived from the Tm C-terminal region ($Tm_{220-284(W269)}$). We also show by NMR spectroscopy that Mg^{2+} binds at the vicinity of His276 in the $Tm_{220-284(W269)}$ fragment and in a shorter peptide, $Tm_{259-284(W269)}$, derived from the last 27 residues of Tm. These observations, when interpreted in light of our previous mutagenesis data[15] and the previously published NMR structures of the Tm C-terminus,[16,17] support a hypothesis that a Mg^{2+} binding site is located at the Tm C-terminus close to the head-to-tail overlapping region at which several polar residues (S271, E272, E273, D275, N279, D280) could contribute to Mg^{2+} binding.

MATERIALS AND METHODS

Construction of Expression Vectors for Tm Fragment Production and Purification

The plasmid vector coding for full length nonfusion recombinant chicken skeletal α-Tm (nfTmW269)[18] and its expression and purification were described previously.[18] The plasmid vector for the expression of the $Tm_{220-284(W269)}$ fragment was constructed by amplifying the sequence corresponding to residues 220-284 using the vector pETMAS269W[18] as a template. The following oligonucleotides were used in the polymerase chain reaction (PCR): *Nde*M219 (5′-TCG CAG AAA CAT ATG AAA TAT GAA GAG-3′) and *Eco*RI(−) (5′-CAT TAA CCT ATA AAA ATA GGC G-3′). The PCR product was digested with *Nde*I and *Eco*RI and ligated into vector pET3a.[19] $Tm_{220-284(W269)}$ was expressed and purified as described.[18,20]

Recombinant $Tm_{259-284(W269)}$ was produced initially as a fusion ($ASTm_{1-21/259-284(W269)}$) of the first 23 residues ($ASTm_{1-21}$) and the last 26 residues ($Tm_{259-284(W269)}$) of ASTm269W[18] separated by a His-tag sequence (6x His) and a thrombin proteolytic recognition site (GSLVPRGS). The plasmid vector for the expression of this fusion was constructed by first amplifying the sequence corresponding to residues 1-21 with an Ala-Ser N-terminal fusion ($ASTm_{1-21}$) using the vector pETMAS269W[18] as a template using the following oligonucleotides in a PCR: *Nde*M (5′-TTT TTT CAT ATG GCT AGC ATG GAT GCC ATC AAG-3′) and *BamHI*21(−) (5′-AAA AGG ATC CAT GAT GAT GAT GAT GAT GTC TGT CCA AGG CAT T-3′). Next, the pair of oligonucleotides *BamHI*259 (5′-TTT T*GG ATC CCT GGT GCC GCG CGG CAG C*GA GCT TTA TGC TCA G-3′) and *Eco*RI(−) (5′-TTT TTT GAA TTC TTA TAT GGA AGT CAT ATC GTT-3′) was used to amplify the C-terminal half ($Tm_{259-284(W269)}$) of Tm using the vector pETMAS269W[18] as a template. The PCR product of the first reaction was cleaved with *Nde*I and *Bam*HI, whereas the product of the second reaction was digested with *Bam*HI and *Eco*RI. A mixture (1:1) of both inserts was simultaneously ligated into the same pET3a vector previously digested with *Nde*I and *Eco*RI.

For expression of the protein fusion ($ASTm_{1-21/259-284(W269)}$), we used *Escherichia coli* strain BL21(DE3).[19] A single colony from a fresh plate was inoculated into 3 mL of 2 × TY medium (16 g/L tryptone, 10 g/L yeast extract, 5 g/L NaCl, pH 7.4) with 100 μg/mL of ampicillin and grown for 5 h at 37°C. A volume of 1.2 mL of cultured cells were inoculated in 2 L of unlabeled modified M9 medium (12.8 g/L Na_2HPO_4-$7H_2O$, 3 g/L KH_2PO_4, 0.84 g/L NaCl, 0,25 g/L NH_4Cl, 100 μM $CaCl_2$, 2 m*M* $MgCl_2$, 40 mg/L $C_6H_{12}O_6$) and grown to an $OD_{600\ nm}$ of 0.8. The cells were collected by centrifugation and resuspended in 2 L of M9 medium containing 0.5 g/L $^{15}NH_4Cl$, 0.4 m*M* IPTG and 100 μg/mL ampicillin or 0.5 g/L $^{15}NH_4Cl$, 2 g/L $^{13}C_6H_{12}O_6$, 0.4 m*M* IPTG, and 100 μg/mL ampicillin for production of single and double isotopically labeled proteins, respectively. Cells were grown for 3.5 h before harvesting and storage at −20°C. Cell lysis was performed in 30 mL of 50 m*M* Tris–HCl (pH 8.0), 25% (w/v) sucrose, 1 m*M* EDTA in a French pressure cell press (16,000 p.s.i.). The lysate was cleared (12,100*g*, 45 min, 4°C), and the protein was found in the insoluble fraction. The protein was solubilized using the above buffer supplemented with 8 *M* urea. This solution was centrifuged (12,100*g*, 15 min, 4°C) and the supernatant collected. Solid ammonium sulfate was added to 50% saturation and the preparation was stirred for 30 min at 25°C. After a second centrifugation (12,100*g*, 30 min, 4°C), solid ammonium sulfate was added again to the supernatant to 90% saturation. Precipitated proteins were collected (12,100*g*, 30 min, 4°C), resuspended in 10 mL of 50 m*M* Tris–HCl (pH 7.0), 1 m*M* EDTA, 100 m*M* KCl, and 8 *M* urea. The proteins were loaded onto a Hiload™ Superdex 75 column equilibrated with the same buffer (1 mL/min, room temperature). $ASTm_{1-21/259-284(W269)}$ fractions were pooled and dialyzed against water. Protein was subsequently lyophilized and resuspended in 5 mL of thrombin cleavage buffer (20 m*M* Tris–HCl (pH 8.4), 150 m*M* NaCl, 2.5 m*M* $CaCl_2$). A volume of 2 mL of thrombin covalently bounded to agarose resin (Thrombin CleanCleave™ kit, Sigma) was added to the protein solution. This mixture was maintained at room temperature with gentle agitation during 16 h. Resin was harvested by centrifugation (4000 rpm, 25°C) and the supernatant containing digested protein collected and loaded into a 1 mL Ni^{2+} Hi-Trap Chelating column previously equilibrated with the thrombin cleavage buffer. The column was washed with 15 mL of cleavage buffer to remove unbound

proteins. During this step, the C-terminal half ($Tm_{259-284}$) was eluted. This fragment carries a Gly-Ser N-terminal extension derived from the thrombin cleavage site. The N-terminal half ($ASTm_{1-21}$) was eluted on addition of 5 mL of cleavage buffer containing 0.8 *M* imidazole. The N- and C-terminal fragments were dialyzed against water using a Spectra/Por dialysis membrane (MWCO: 1,000) and lyophilized. The $ASTm_{1-21}$ fragment was unstable and degraded during dialysis. Protein concentrations were determined as described.[21]

Proteolysis Analysis

Nonpolymerizable full-length Tm (nfTmW269)[18] (5 μM dimer) was dissolved in four different buffers: (i) 25 m*M* MOPS (pH 7.0), 5 m*M* $MgCl_2$, 1 m*M* DTT; (ii) 54.5 m*M* MOPS (pH 7.0), 0.5 m*M* EDTA, 1 m*M* DTT; (iii) 25 m*M* MOPS (pH 7.0), 100 m*M* NaCl, 5 m*M* $MgCl_2$, 1 m*M* DTT; (iv) 54.5 m*M* MOPS (pH 7.0), 100 m*M* NaCl, 0.5 m*M* EDTA, 1 m*M* DTT. Each reaction was started by adding α-chymotrypsin to a final concentration of 1 μg/mL and was terminated by adding phenylmethanesulfonyl fluoride (PMSF) to a final concentration of 1 m*M*. The products of the digestion reactions were analyzed by 15% SDS-PAGE stained with Comassie Brilliant Blue.

Circular Dichroism Spectroscopy

nfTmW269 (5 μM dimer) was dissolved in 25 m*M* MOPS (pH 7.0), 100 m*M* NaCl, 5 m*M* $MgCl_2$, 1 m*M* DTT, or 54.5 m*M* MOPS (pH 7.0), 100 m*M* NaCl, 0.5 m*M* EDTA, 1 m*M* DTT. Temperature dependence of circular dichroism (CD) was monitored at 222 nm at 2°C intervals from 4°C to 80°C and back to 4°C at a velocity of 1°C/min in a Jasco-720 spectropolarimeter (Jasco, Tokyo, Japan). In the case of $Tm_{220-284(W269)}$, protein (10 μM) was dissolved in four different buffers: 25 m*M* MOPS (pH 7.0), 5 m*M* $MgCl_2$, 1 m*M* DTT; 54.5 m*M* MOPS (pH 7.0), 0.5 m*M* EDTA, 1 m*M* DTT; 25 m*M* MOPS (pH 7.0), 100 m*M* NaCl, 5 m*M* $MgCl_2$, 1 m*M* DTT; 54.5 m*M* MOPS (pH 7.0), 100 m*M* NaCl, 0.5 m*M* EDTA, 1 m*M* DTT. The measurements were collected as described for nfTmW269.

Nuclear Magnetic Resonance Measurements

NMR samples were prepared containing isotopically labeled $Tm_{259-284(W269)}$ 0.2-0.3 m*M* (dimer) in 25 m*M* sodium phosphate (pH 7.0), 5% D_2O at 10°C. Data were collected on a Varian INOVA 600 MHz (AS600/51) spectrometer using a cryogenic triple-resonance probehead equipped with z-axis pulse field gradient or in a Bruker Avance III 800 MHz spectrometer equipped with a TXI probe. Measurements were performed in Shigemi D_2O matched NMR tubes (Shigemi). All the spectra were processed and analyzed using the NMRPipe/NMRDraw software package.[22] The CcpNMR Analysis program suite was used for analyses of spectra.[23]

To assign backbone sequence-specific ^1H, ^{15}N, and ^{13}C resonances, we used a set of triple resonance NMR spectra: HNCACB,[24] HNCA,[25,26] CBCA(CO)NH,[27] HNCO,[25,26] HN(CO)CA.[26,28] Triple-resonance experiments were typically acquired as matrices of 1024 × 140 × 128 complex points in the ^1H, ^{13}C and ^{15}N dimensions. The 3D ^1H-^{15}N TOCSY-HSQC spectrum[29] using a TOCSY mixing time of 80 ms was used to assign the ^1H resonances from the side-chains. 3D ^1H-^{15}N NOESY-HSQC[30–32] spectra with mixing times of 120 ms were used to confirm sequence-specific resonance assignments and to establish short, medium, and long-range NOE connectivities.

$Tm_{259-284(W269)}$ was also dissolved in 25 m*M* sodium phosphate (pH 7.0), 42 m*M* NaCl or 25 m*M* sodium phosphate (pH 7.0), 14 m*M* $MgCl_2$. ^1H-^{15}N HSQC spectra were collected for both samples at different temperatures (10, 15, 20, 25, 30°C) to follow specific changes in the spectra caused by the binding of the Mg^{2+} ion. The same samples were lyophilized and resuspended in D_2O. ^1H-^{13}C HSQC spectra of $Tm_{220-284(W269)}$ and $Tm_{259-284(W269)}$ in the region of the aromatic resonances were collected to follow specific changes in the aromatic carbons upon Mg^{2+} binding.

We carried out measurements of backbone ^{15}N longitudinal (R_1) and transversal (R_2) relaxation rates and steady-state heteronuclear NOE (HNOE) using the Biopack (Varian) implementations of pulse sequences performed as described in Refs. 33 and 34. $Tm_{259-284(W269)}$ (0.3 m*M* dimer) was dissolved in 25 m*M* sodium phosphate (pH 7.0) at 10°C. Thirteen spectra were recorded in order to measure R_1 relaxation rates with delays (t) of: 50, 150, 250, 350, 450, 550, 650, 750, 850, 1050, 1250, 1650, 1850 ms, whereas 10 spectra with relaxation delays (t) of: 30, 70, 110, 150, 190, 230, 270, 310, 350, 410 ms were recorded to measure R_2. The cross-peak intensities were fit to a two-parameter single exponential decay function:

$$I(t) = I_o \exp(-Rt) \quad (1)$$

where $I(t)$ is the cross-peak intensity at time t, I_o is the initial cross-peak intensity at $t = 0$ and R is R_1 or R_2 relaxation rates. Fitting and parameter estimation was performed using the nonlinear least square algorithm implemented in GNUPLOT 4.0 (www.gnuplot.info). Error estimates for peak intensities were taken from the noise level in the spectra. Estimates for decay rate errors were taken from the standard errors given by GNUPLOT. The HNOE was calculated from the ratio of cross-peak intensities in two spectra recorded with (I_{sat}) or without (I_{unsat}) amide proton saturation during the relaxation delay of 3 seconds.

RESULTS AND DISCUSSION

Mg^{2+} Stabilizes Tm Structure

The α-Tm amino acid sequence is rich in negatively charged residues, which are clustered along the molecule (see Figure 1). It may be expected that repulsive interactions between those residues could create regions of local instability in the protein. Indeed, the α-helical conformation of full-length Tm or its fragments are stabilized at high ionic strength conditions,[35–38] which possibly increases the stability of the coiled-coil by reducing charge–charge and dipole–dipole repulsive interactions while at the same time enhancing apolar–apolar interactions.[37] In a previous study, we showed that the addition of Mg^{2+} induced a remarkable increase in the thermal stability of two fragments corresponding to the N- and C-terminal halves of Tm,[15] suggesting that Mg^{2+} binds to both fragments. Furthermore, when mutations in the head-to-tail

MDAIKKK MQMLKLD KENALDR AEQAEAD KKAAEER SKQLEDE LVALQKK LKGTEDE LDKYSES
LKDAQEK LELADKK ATDAESE VASLNRR IQLYEEE LDRAGER LATALQK LEEAEKA ADESERG
MKVIENR AQKDEEK MEIQEIQ LKEAKHI AEEADRK YEEVARK LVIIEGD LERAEER AELSESK
CAELEEE LKTVTNN LKSLEAQ AEKYSQK EDKYEEE IKVLTDK LKEAETR AEFAERS VTKLEKS
IDDLEDE LYAQKLK YKAISEE LDHALND MTSI

FIGURE 1 Primary structure of chicken skeletal α-tropomyosin. Acidic residues (bold) are clustered along the sequence. The sequence of $Tm_{220\text{-}284(W269)}$ (residues: 220–284) is underlined, while the sequence of $Tm_{259\text{-}284(W269)}$ (residues: 259–284) is doubly underlined.

overlap region were tested, differences in Mg^{2+} induced stability gains were only observed with the C-terminal mutants (D275A, H276A, H276E, and D280A), but not for N-terminal mutants (D2A, K5A, K6A, and K7A). These observations suggest that one or more specific Mg^{2+} binding site could be located in the C-terminal portion of the head-to-tail overlap region.

To further investigate the effects of Mg^{2+} binding to Tm, we first studied its effect on the structure and stability of nonpolymerizable full-length recombinant Tm ($nfTm_{W269}$). Proteolytic enzymes can be used to probe changes within Tm structure.[36,39] Limited proteolytic digestions with α-chymotrypsin were performed to detect local stability changes caused by the addition of Na^+ and/or Mg^{2+} ions (see Figure 2). In the absence of Mg^{2+}, the presence of 100 m*M* NaCl caused a decrease in the cleavage rate of Tm by chymotrypsin. These results are consistent with previous observations that Tm is more stable in high salt conditions[35–39] and that Tm becomes increasingly resistant to trypsin attack when ionic strength is raised.[36] The time course of the proteolysis reaction (15, 30, 45 min at 37°C; Figure 2) shows that on addition of Mg^{2+} Tm becomes more stable in both the presence or absence of 100 m*M* NaCl.

Figure 3A shows that addition of Mg^{2+} also causes a slight increase in the thermal stability of $nfTm_{W269}$ (1.6°C). These CD thermal denaturation profiles were collected in the presence of 100 m*M* NaCl, where the denaturation transition is reversible and the Tm structure is already significantly stabilized in relation to low ionic strength conditions.[37] Although we did not observe protein aggregation on Mg^{2+} addition in the absence of NaCl, the thermal denaturation curves were not reversible under these low ionic strength conditions and Tm aggregates appeared during the cooling step (80°C → 4°C) of denaturation experiments (data not shown). These results are consistent with previous work by Ishi and Lehrer[40] who studied the formation of Tm paracrystals induced by Mg^{2+} in a series of experiments where pH, salt and temperature were varied. They observed that at low concentrations (<15 mM) Mg^{2+} favors Tm paracrystal formation, while at high concentrations (>15 mM) it inhibits this process and that addition of NaCl slowed protein aggregation.[40]

Mg^{2+} Binds to the C-Terminal Region of Tm

We then investigated the effect of Mg^{2+} on the stability of a recombinant fragment corresponding to the last 65 residues of the Tm molecule ($Tm_{220\text{-}284(W269)}$). Although this peptide is less stable than longer C-terminal Tm fragments,[35,41] it has been shown to interact with a Tm N-terminal fragment to form the head-to-tail complex.[38] Initially, we

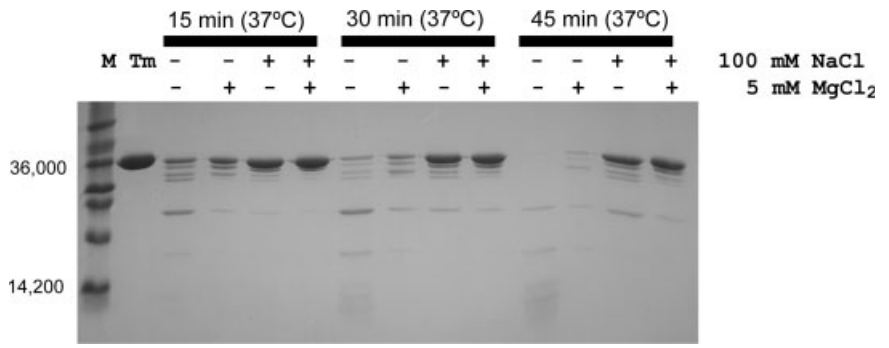

FIGURE 2 Proteolytic digestion of nfTmW269 by α-chymotrypsin. M: Molecular mass marker (14,000–70,000 Da); lane 1: 5 μM nfTmW269; lane 2, 6, 10: 5 μM nfTmW269, 54.5 m*M* MOPS (pH 7.0), 0.5 m*M* EDTA, 1 m*M* DTT; lane 3, 7, 11: 5 μM nfTmW269, 25 m*M* MOPS (pH 7.0), 5 m*M* $MgCl_2$, 1 m*M* DTT; lane 4, 8, 12: 5 μM nfTmW269, 54.5 m*M* MOPS (pH 7.0), 100 m*M* NaCl, 0.5 m*M* EDTA, 1 m*M* DTT; lane 5, 9, 13: 5 μM nfTmW269, 25 m*M* MOPS (pH 7.0), 100 m*M* NaCl, 5 m*M* $MgCl_2$, 1 m*M* DTT. Aliquots of the digestion mixture were collected at three different times: 15 min, 30 min, and 45 min at 37°C.

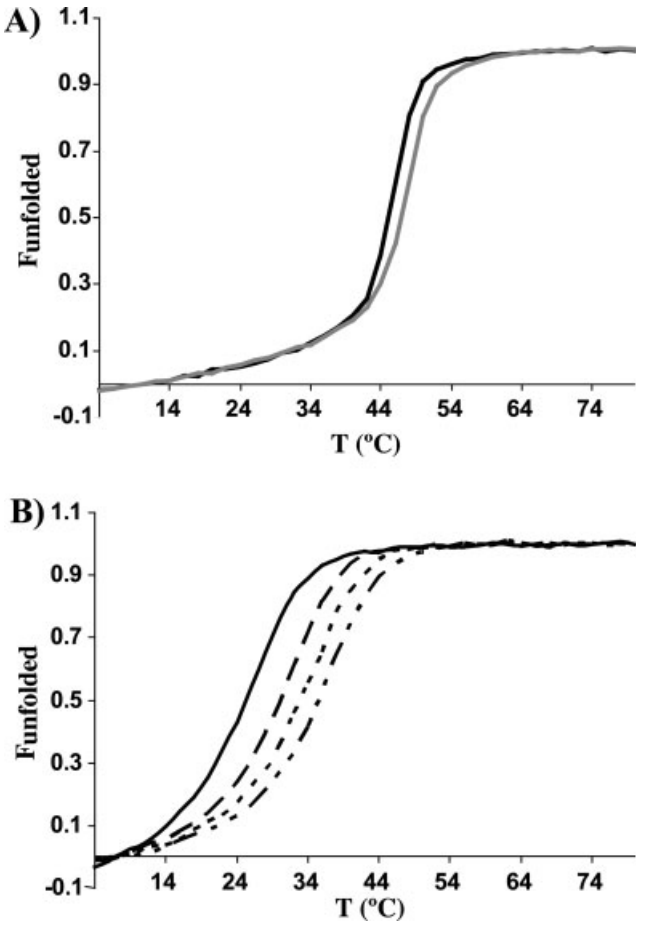

FIGURE 3 Thermal denaturation curves of nfTmW269 and $Tm_{220\text{-}284(W269)}$. Unfolded fraction is plotted as a function of temperature. A, Thermal denaturation profiles of nfTmW269 in 54.5 m*M* MOPS (pH 7.0), 100 m*M* NaCl, 0.5 m*M* EDTA, 1 m*M* DTT (T_m: 44.5°C) (black) or 25 m*M* MOPS (pH 7.0), 5 m*M* $MgCl_2$, 100 m*M* NaCl, 1 m*M* DTT (T_m: 46.1°C) (gray). Protein concentration: 5 μM (dimer). B, Thermal denaturation profiles of $Tm_{220\text{-}284(W269)}$ in: 54.5 m*M* MOPS (pH 7.0), 0.5 m*M* EDTA, 1 m*M* DTT (———) (T_m: 23.9°C); 54.5 m*M* MOPS (pH 7.0), 100 m*M* NaCl, 0.5 m*M* EDTA, 1 m*M* DTT (— — —) (T_m: 29.2°C); 25 m*M* MOPS (pH 7.0), 100 m*M* NaCl, 5 m*M* $MgCl_2$, 1 m*M* DTT (------) (T_m: 31.9°C); 25 m*M* MOPS (pH 7.0), 5 m*M* $MgCl_2$, 1 m*M* DTT (— - — - -) (T_m: 34.3°C). Protein concentration: 10 μM (dimer).

studied the effect of Mg^{2+} binding in the thermal stability of $Tm_{220\text{-}284(W269)}$. Different from what was observed with full-length Tm, the addition of Mg^{2+} did not induce protein aggregation in the absence of 100 m*M* NaCl; this allowed us to obtain fully reversible thermal denaturation curves. Figure 3B shows thermal denaturation profiles of this fragment in 0 or 100 m*M* NaCl in the presence or absence of 5 m*M* Mg^{2+}. The simple addition of 100 m*M* NaCl in the absence of Mg^{2+} resulted in an increase in the stability of $Tm_{220\text{-}284(W269)}$ ($\Delta T_m = 5.3$°C). This result agrees with a previous study, which showed that addition of 100 m*M* KCl increased its α-helical content from 32% to 48%.[38] However, a larger gain in stability is observed upon the addition of 5 m*M* Mg^{2+} in the absence of NaCl ($\Delta T_m = 10.4$°C) (Figure 3B). Furthermore, in the presence of 5 m*M* $MgCl_2$, the addition of 100 m*M* NaCl destabilizes the fragment. These results indicate that NaCl and $MgCl_2$ stabilize the structure of this Tm C-terminal fragment in fundamentally different ways,

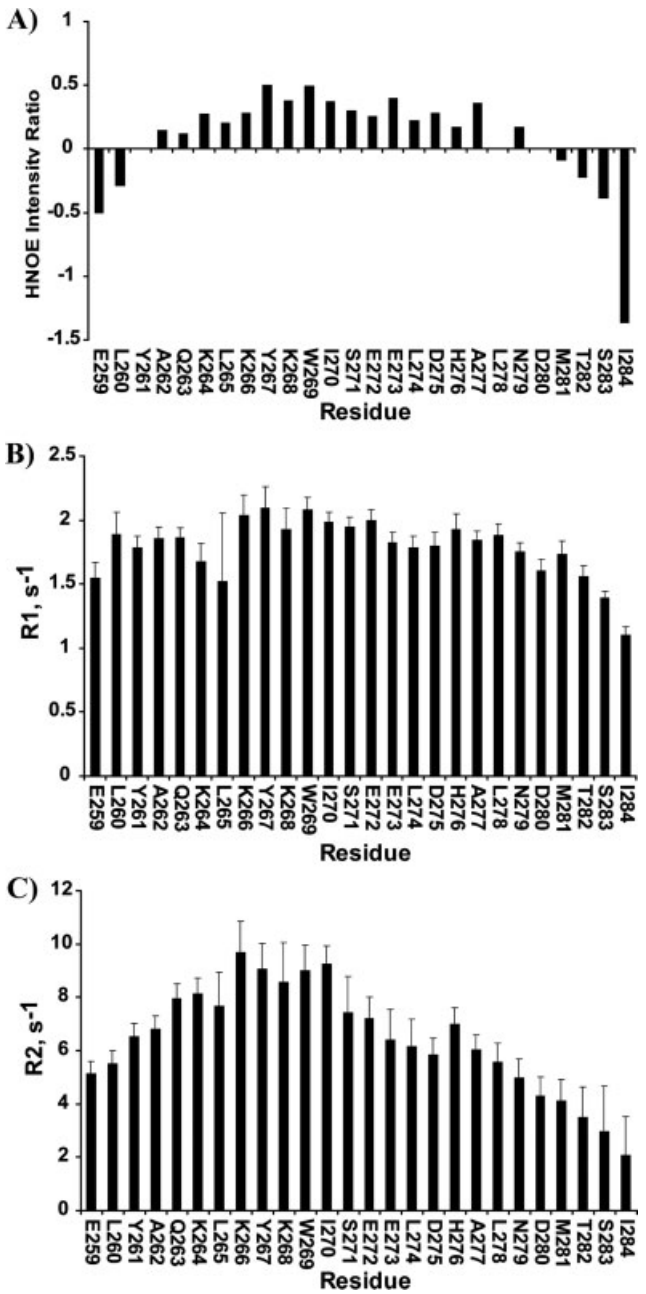

FIGURE 4 Backbone 15N heteronuclear relaxation data of $Tm_{259\text{-}284(W269)}$ at 600 MHz. A, {1H}-15N Heteronuclear NOE (HNOE). B, Longitudinal relaxation rate (R1, s-1). C, Transversal relaxation rate (R2, s-1). Conditions: 0.3 m*M* (dimer) $Tm_{259\text{-}284(W269)}$, 25 m*M* sodium phosphate (pH 7.0), at 10°C.

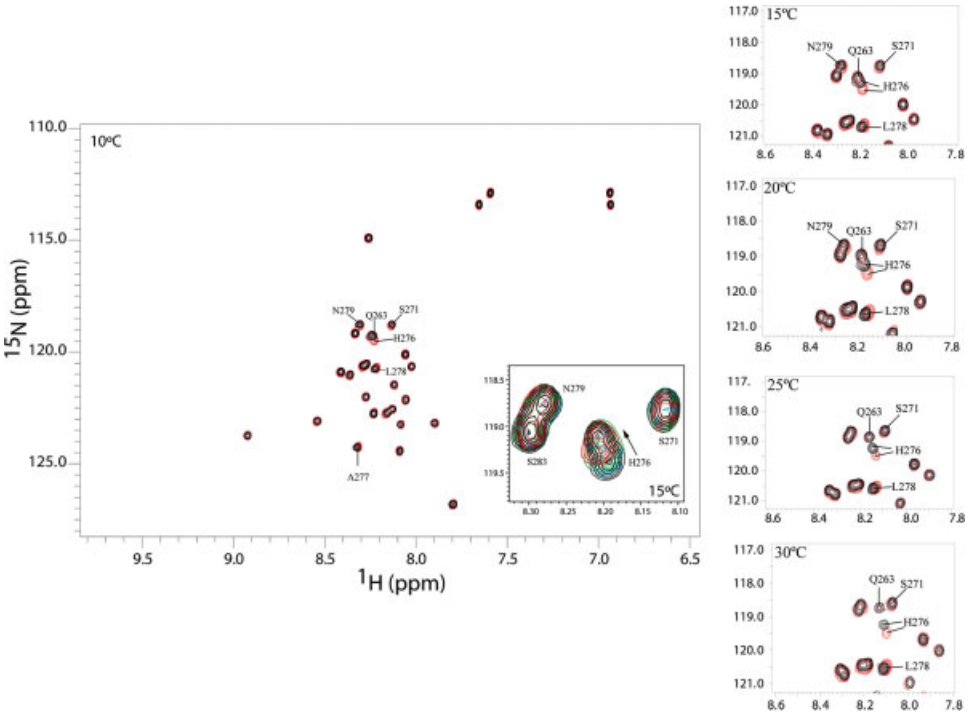

FIGURE 5 ^{1}H-^{15}N HSQC spectra of 15N $Tm_{259\text{-}284(W269)}$ in the absence (red) and presence of Mg^{2+} (black) at different temperatures. The indicated cross-peaks are labeled with the residue number corresponding to chicken striated muscle α-Tm sequence. The labeled peaks presented the most significant shifts upon ion addition. The effect of temperature (from 10°C to 30°C) on the ^{1}H-^{15}N HSQC spectra is shown in the panels to the right. The protein concentration was 0.25 m*M* (dimer) in 25 m*M* sodium phosphate (pH 7.0) with 42 m*M* NaCl or 14 m*M* $MgCl_2$. The inset shows the spectral region of H276 in ^{1}H-^{15}N HSQC spectra of $Tm_{259\text{-}284(W269)}$ acquired in the absence (black) or in the presence of 1.3 (cyan), 4.0 (green), and 8.0 m*M* $MgCl_2$ (magenta) in 25 m*M* sodium phosphate (pH 7.0) and 38 m*M* NaCl at 15°C.

which may in fact be mutually exclusive. It has been observed that divalent cations can bind to regions rich in negatively charged residues in which they mediate salt bridge interactions between acidic side chains.[42–46] In this way, Mg^{2+} binding would have the effect of converting repulsive interactions into attractive ones, leading to large increments in protein stability.[44,46] Other reports have suggested that Na^{+} can interfere with Mg^{2+} binding by shielding electrostatic interactions, rather than competing for specific sites.[40,47]

A Flexible Peptide Corresponding to the Last 26 Residues of Tm Presents Residual Structure in the Central Region

Though $Tm_{220\text{-}284(W269)}$ is a relatively small polypeptide (65 amino acids in each monomer) with dimer molecular weight of ∼14 kDa, its ^{1}H-^{15}N HSQC spectrum displays extensive peak broadening. This prevented us from proceeding with the NMR studies of this fragment. Therefore, we produced a smaller recombinant peptide corresponding to the last 26 aminoacids from the C-terminal region ($Tm_{259\text{-}284(W269)}$). This fragment carries a Gly-Ser N-terminal extension derived from the thrombin cleavage site used during its production (see Materials and Methods section). The $Tm_{259\text{-}284(W269)}$ HSQC spectrum shows sharp linewidths and well resolved peaks (see Figure 5 below). The CD spectrum of $Tm_{259\text{-}284(W269)}$ shows low residual ellipticity at 222 nm indicative of little α-helical content (data not shown). A similar-sized fragment derived from the Tm C-terminus (residues 253–280) also displayed very little α-helix content even at low temperatures and high concentrations.[48,49]

NMR spectroscopy can provide more detailed conformational information regarding residual structure present in unfolded polypeptides.[50] Figure 4 shows backbone ^{15}N R_1 and R_2 relaxation rates and steady state {^{1}H}-^{15}N NOE data obtained for $Tm_{259\text{-}284(W269)}$ as a function of the amino acid sequence. The R_1 rates show little variation along the peptide sequence ($1.8 \pm 0.2\ s^{-1}$), while R_2 and NOE are lower at the

termini but increase at the central residues that display average values of 8.4 ± 0.8 s^{-1} (R_2) (residues Q263–E272) and 0.3 ± 0.1 (NOE) (residues A262–N279), respectively. We note that the ^{15}N R_2 rates at the center of the peptide are larger than those observed in unfolded proteins lacking residual secondary structure, typically 3 s^{-1}.[50] The above observations suggest that, although the peptide is highly flexible and does not present medium range NOEs in the NOESY spectra (data not shown), it has some residual structure in the central region.

Localization of a Putative Mg^{2+} Binding Site at the Tm C-Terminal Region

Addition of Mg^{2+} to the $Tm_{259\text{-}284(W269)}$ sample induced specific changes in the ^1H-^{15}N HSQC spectrum at pH 7.0 (see Figure 5). The cross-peaks corresponding to residues S271, H276, A277, L278, and N279 experienced shifts upon addition of Mg^{2+}, indicative of ion binding (see Figure 5). Comparison of the spectra in the absence and presence of Mg^{2+} at different temperatures (10°C–30°C) shows that Mg^{2+} continues to bind at elevated temperatures and that the most significant changes occurred for the H276 amide cross-peak (see Figure 5). When different Mg^{2+} concentrations were tested, the H276 amide cross-peak experienced significant shifts at 4 m*M* or greater (see Figure 5). No changes in the ^1H-^{15}N HSQC spectrum of $Tm_{259\text{-}284(W269)}$ were observed upon titrating Mg^{2+} at a lower pH, 5.5 (data not shown).

Analysis of ^1H-^{13}C HSQC spectra in the region of the aromatic resonances show that Mg^{2+} binding causes a shift in the position of the $^1H^{\varepsilon 1}$-$^{13}C^{\varepsilon 1}$ cross-peak of the H276 side chain in $Tm_{259\text{-}284(W269)}$ (Figure 6A). Because the unstructured nature of $Tm_{259\text{-}284(W269)}$ puts into question the relevance of its interaction with Mg^{2+}, we looked for similar changes in the larger well-folded $Tm_{220\text{-}284(W269)}$ coiled-coil. Figure 6B shows that a similar, though less marked, shift is also observed in the ^1H-^{13}C HSQC of the $Tm_{220\text{-}284(W269)}$ fragment. These observations indicate that Mg^{2+} is binding to the same region of both the larger and the smaller fragments.

Although none of the residues which displayed cross-peak shifts in the HSQC spectra are negatively charged (S271, H276, A277, L278, N279), they are located in a region of very high negative charge density containing several potential Mg^{2+} binding residues (E272, E273, D275, and D280). It is possible that Mg^{2+} induces a resampling of side chain rotamer conformations in this region of the molecule, which would explain why the greatest ion-induced perturbations are observed for H276 and some of the neighboring residues (S271, A277, L278, N279) (see Figure 8).

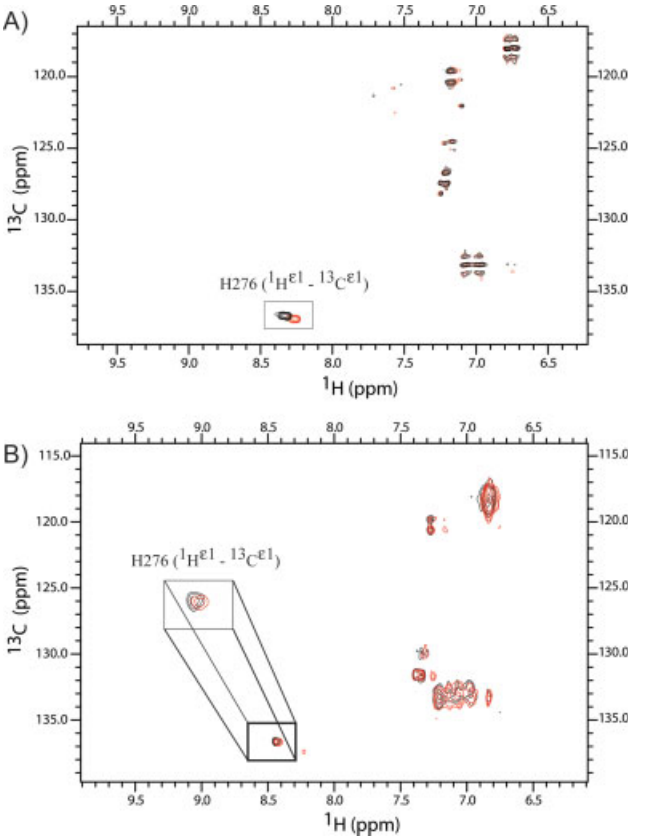

FIGURE 6 ^1H-^{13}C HSQC spectra of uniformly $^{15}N/^{13}C$-labeled Tm fragments in the region of the aromatic carbons. A, ^1H-^{13}C HSQC spectra of $Tm_{259\text{-}284(W269)}$ fragment in the absence (red) and presence of Mg^{2+} (black). The significant shift observed for the His276 side chain $^1H^{\varepsilon 1}$-$^{13}C^{\varepsilon 1}$ peak correlation is indicated. B, ^1H-^{13}C HSQC spectra of $Tm_{220\text{-}284(W269)}$ in the absence (red) and presence of Mg^{2+} (black). A similar shift of the $^1H^{\varepsilon}$-$^{13}C^{\varepsilon 1}$ cross peak of His276 is also observed upon Mg^{2+} ion addition. The box shows an amplification of the spectral region of this cross peak. Conditions: $Tm_{220\text{-}284(W269)}$ concentration: 0.16 m*M* (dimer); $Tm_{259\text{-}284(W269)}$ concentration: 0.25 m*M* (dimer); 25 m*M* sodium phosphate (pH 7.0), 42 m*M* NaCl or 14 m*M* $MgCl_2$, at 10°C.

CONCLUSIONS

We studied the interaction between Mg^{2+} and full-length Tm and smaller fragments corresponding to the last 65 and 27 Tm residues. Although the smaller Tm peptide ($Tm_{259\text{-}284(W269)}$) is flexible and to large extent unstructured, relaxation measurements indicate that the central region retains some residual structure (see Figure 4). The stability of the larger $Tm_{220\text{-}284(W269)}$ fragment increases significantly in the presence of Mg^{2+} and through a mechanism significantly different from that observed for Na^+. Mg^{2+} stabilizes the helical conformation of both N- and C-terminal halves of the Tm molecule[15] probably by binding to multiple sites made of clusters of acidic residues. NMR analysis shows that Mg^{2+} induces chemical shift perturbations in both $Tm_{220\text{-}284(W269)}$ and $Tm_{259\text{-}284(W269)}$

in the vicinity of His276 and that this may therefore represent one Mg^{2+} binding site. This hypothesis is consistent with previous studies that showed that mutations introduced at the extreme C-terminal region (but not the N-terminus) modulates the Mg^{2+}-induced gain in Tm stability.[15]

We thank Dr. Ana Carolina Zeri and the Laboratório Nacional de Luz Síncontron (LNLS) for conceding machine time on the Varian Inova 600 MHz NMR spectrometer, and Dr. Fabio Almeida and Ana P. Valente (Universidade Federal do Rio de Janeiro) for conceding NMR time at the Bruker Avance III 800 MHz spectrometer.

REFERENCES

1. Potter, J. D.; Gergely, J. J Biol Chem 1975, 250, 4628–4633.
2. Leavis, P. C.; Rosenfeld, S. S.; Gergely, J.; Grabarek, Z.; Drabikowski, W. J Biol Chem 1978, 253, 5452–5459.
3. Zot, H. G.; Potter, J. D. J Biol Chem 1982, 257, 7678–7683.
4. Kabsch, W.; Mannherz, H. G.; Suck, D.; Pai, E. F.; Holmes, K. C. Nature 1990, 347, 37–44.
5. Egelman, E. H.; Orlova, A. Curr Opin Struct Biol 1995, 5, 172–180.
6. Farah, C. S.; Reinach, F. C. FASEB J 1995, 9: 755–767.
7. Gordon, A. M.; Homsher, E.; Regnier, M. Physiol Rev 2000, 80, 853–924.
8. Perry, S. V. J Muscle Res Cell Motil 2001, 23, 353–361.
9. Stewart, M.; McLahlan, A. D. Nature 1975, 275, 331–333.
10. McLachlan, A. D.; Stewart, M. J Mol Biol 1976, 103, 251–269.
11. Yang, Y. Z.; Korn, E. D.; Eisenberg, E. J Biol Chem 1979, 254, 7137–7140.
12. Cote, G. P.; Smillie, L. B. J Biol Chem 1981, 256, 7257–7261.
13. Cho, Y. J.; Liu, J.; Hitchcock-DeGregori, S. E. J Biol Chem 1990, 265, 538–545.
14. Lorenz, M.; Poole, K. J. V.; Popp, D.; Rosenbaum, G.; Holmes, K. C. J Mol Biol 1995, 246, 108–119.
15. Corrêa, F.; Salinas, R. K.; Bonvin, A. M. J. J.; Farah, C. S. Proteins 2008, 73, 902–917.
16. Greenfield, N. J.; Swapna, G. V. T.; Huang, Y.; Palm, T.; Graboski, S.; Montelione, G. T.; Hitchcock-DeGregori, S. E. Biochemistry 2003, 42, 614–619.
17. Greenfield, N. J.; Huang, Y. J.; Swapna, G. V. T.; Bhattachrya, A.; Rapp, B.; Singh, A.; Montelione, G. T.; Hitchcock-DeGregori, S. E. J Mol Biol 2006, 364, 80–96.
18. Sousa, A. D; Farah, C. S. J Biol Chem 2002, 277, 2081–2088.
19. Studier, F. W.; Rosenberg, A. H.; Dunn, J. J.; Dubendorff, J. W. Methods Enzymol 1990, 185, 60–89.
20. Farah, C. S.; Reinach, F. C. Biochemistry 1999, 38, 10543–10551.
21. Hartree E. F. Anal Biochem 1972, 48, 422–427.
22. Delaglio, F.; Grzesiek, S.; Vuister, G. W.; Zhu, G.; Pfeifer, J.; Bax, A. J Biomol NMR 1995, 6, 277–293.
23. Vranken, W. F.; Boucher, W.; Stevens, T. J.; Fogh, R. H.; Pajon, A.; Llinas, M.; Ulrich, E. L.; Markley, J. L.; Ionides, J.; Laue, E. D. Proteins 2005, 59, 687–696.
24. Wittekind, M.; Mueller, L. J Magn Reson Ser B 1993, 101, 201–205.
25. Kay, L. E; Ikura, M.; Tschudin, R.; Bax, A. J Magn Reson 1990, 89, 496–514.
26. Grzesiek, S.; Bax, A. J Magn Reson 1992, 96, 432–440.
27. Grzesiek, S.; Bax, A. J Am Chem Soc 1992, 114, 6291–6293.
28. Bax, A.; Ikura, M. J Biomol NMR 1991, 1, 99–104.
29. Clore, G. M.; Bax, A.; Gronenborn, A. M. J Biomol NMR 1991, 1, 13–22.
30. Marion, D.; Driscoll, P. C.; Kay, L. E.; Wingfield, P. T.; Bax, A.; Gronenborn, A. M.; Clore, G. M. Biochemistry 1989, 28, 6150–6156.
31. Marion, D.; Kay, L. E.; Sparks, S. W.; Torchia, D. A.; Bax, A. J Am Chem Soc 1989, 111, 1515–1517.
32. Zuiderweg, E. R. P.; Fesik, S. W. Biochemistry 1989, 28, 2387–2391.
33. Kay, L. E.; Nicholson, L. K.; Delaglio, F.; Bax, A.; Torchia, D. A. J Mag Res 1992, 97, 359–375.
34. Kay, L. E.; Torchia, D. A.; Bax, A. Biochemistry 1989, 28, 8972–8979.
35. Paulucci, A. A.; Hicks, L.; Machado, A.; Miranda, M. T. M.; Kay, C. M.; Farah, C. S. J Biol Chem 2002, 277, 39574–39584.
36. Ueno, H. Biochemistry 1984, 23, 4791–4798.
37. Mo, J. M.; Holtzer, M. E.; Holtzer, A. Biopolymers 1990, 30, 921–927.
38. Paulucci, A. A.; Katsuyama, A. M.; Sousa, A. D.; Farah, C. S. Eur J Biochem 2004, 271, 589–600.
39. Sano, K.-I.; Maeda, K.; Taniguchi, H.; Maeda, Y. Eur J Biochem 2000, 267, 4870–4877.
40. Ishii, Y.; Lehrer, S. S. Biophys J 1989, 56, 107–114.
41. Corrêa, F.; Farah, C. S. Biophys J 2007, 92, 2463–2475.
42. Needham, J. V.; Chen, T. Y.; Falke, J. J. Biochemistry 1993, 32, 3363–3367.
43. Oda, Y.; Yamazaki, T.; Nagayama, K.; Kanaya, S.; Kuroda, Y.; Nakamura, H. Biochemistry 1994, 33, 5275–5284.
44. Kanaya, S.; Oobatake, M.; Liu, Y. J Biol Chem 1996, 51, 32729–32736.
45. Ohki, S.; Ikura, M.; Zhang, M. Biochemistry 1997, 36, 4309–4316.
46. Masino, L.; Martin, S. R.; Bailey, P. M. Protein Sci 2000, 9, 1519–1529.
47. Oosawa, F. Polyelectrolytes; Marcel Dekker Inc.: New York, 1971.
48. Holtzer, M. E.; Mints, L.; Angeletti, R. H.; d'Avignon, D. A.; Holtzer, A. Biopolymers 2001, 59, 257–265.
49. Holtzer, M. E.; Crimmins, D. L.; Holtzer, A. Biopolymers 1995, 35, 125–136.
50. Wirmer, J.; Peti, W.; Schwalbe, H. J Biomol NMR 2006, 35, 175–186.

Reviewing Editor: David Wemmer